

Decay rates and survival probabilities in open quantum systems

Sandro Wimberger,^(a,b) Andreas Krug,^(a) and Andreas Buchleitner^(a)

^(a)Max-Planck-Institut für Physik komplexer Systeme, Nöthnitzer Str. 38, D-01187 Dresden

^(b)Università degli Studi dell' Insubria, Via Valleggio 11, I-22100 Como

(March 30, 2022)

We provide the first statistical analysis of the decay rates of strongly driven 3D atomic Rydberg states. The distribution of the rates exhibits universal features due to Anderson localization, while universality of the time dependent decay requires particular initial conditions.

PACS numbers: 05.45.Mt, 32.80Rm, 42.50Hz, 72.15Rn

The macroscopic transport properties of classical and quantum systems sensitively depend on the dynamics of their microscopic constituents. Whereas regular Hamiltonian dynamics implies the quasiperiodic confinement of phase space density, chaotic motion and disorder generically induce diffusion-like probability transport exploring all accessible phase space at sufficiently long times. In low-dimensional, disordered quantum systems *Anderson localization* efficiently inhibits diffusive transport through quantum interference, as first predicted by Anderson for the charge transfer across disordered solid state samples. Later on it was realized that chaos can substitute for disorder in Anderson's scenario, leading to *dynamical localization* [1,2] of quantum probability transport. However, as a further complication, quantum systems with classically non-integrable Hamiltonian dynamics (or, in the absence of a clear classical analog, with strongly coupled degrees of freedom) most often do not feature purely chaotic but rather mixed regular chaotic dynamics: besides the chaotic component of phase space the latter also comprises regular regions separated from the chaotic domain by fractal structures like cantori [3]. Hence, dynamically localized quantum transport may be amended by quantum tunneling from regular regions or by semiclassical localization in the vicinity of partial phase space barriers [4].

A rather robust measure of transport is the transmission or decay probability of some initial probability distribution across or from a confined region Ω of phase space. Whereas the transmission problem immediately suggests a scattering approach, decay is most conveniently described by the norm $\| \mathcal{P}_\Omega \cdot U |\phi_0\rangle \|$ of the time evolved initial state $|\phi_0\rangle$ upon projection \mathcal{P}_Ω on the phase space domain we want to characterize. If Ω is confined by an absorbing boundary, attached to some leads which allow for transport to infinity, or coupled to some continuum of states, then $\| \mathcal{P}_\Omega \cdot U |\phi_0\rangle \|$ will decrease monotonically in time, for generic $|\phi_0\rangle$ [5–8]. Given the spectral decomposition of the Hamiltonian, this finite leakage from Ω can be accounted for by associating non-

vanishing (exponential) decay rates Γ_j with eigenstates $|\epsilon_j\rangle$ with non-vanishing support on Ω . Given some initial $|\phi_0\rangle = \mathcal{P}_\Omega |\phi_0\rangle$, the survival probability within the domain Ω boils down to [6]

$$P_{\text{surv}}(t) = \| \mathcal{P}_\Omega \cdot U |\phi_0\rangle \| = \sum_j w_j \exp(-\Gamma_j t). \quad (1)$$

All information on the decay process is now encoded [9] (i) in the set of decay rates – which is a *global* spectral property of the problem – and (ii) in the expansion coefficients $w_j = |\langle \phi_0 | \epsilon_j \rangle|^2$ of the initial wave packet in the eigenbasis, what is a specific representation of the *initial condition*, and a *local* property to the extent that $|\phi_0\rangle$ is localized. With these premises, our initial assertion on the crucial importance of microscopic dynamics for macroscopic transport leads to the guiding question of our present contribution [9,10]: How do classically mixed regular-dynamics affect these global and local spectral properties, and, consequently, the time dependence of P_{surv} ? Whilst, recently, a considerable corpus of literature has addressed this problem within the context of simple models of mesoscopic transport [7,10,11], we shall here underpin our rather general answer by a numerically exact treatment of highly excited three dimensional Rydberg states under strong microwave driving [12]. These are paradigmatic objects to (theoretically and experimentally) study [6,9,12,13] quantum probability decay in the presence of tunneling as well as semiclassical and dynamical localization, and allow a natural and clean definition of P_{surv} and the associated projection \mathcal{P}_Ω , without any approximations.

Let us start with a brief reminder of dynamical localization in periodically driven hydrogen Rydberg atoms, to establish the analogy between the general transport problem depicted above and our specific choice of its physical realization: The atoms are initially prepared in an unperturbed atomic eigenstate $|\phi_0\rangle = |n_0 \ell_0 m_0\rangle$ labeled by the principal quantum number n_0 , the angular momentum ℓ_0 , and the angular momentum projection m_0 . For linearly polarized coherent driving (which we treat in dipole approximation) of amplitude F at frequency ω , m_0 is a good quantum number inherited from the rotational symmetry of the problem, and the atomic excitation process proceeds through the subsequent absorption and/or emission of photons from/into the field, along a sequence of near resonantly coupled states $|n \ell\rangle$. Provided F is large enough compared to the attractive force exerted on the electron by the nucleus, the classical dynamics of the driven Rydberg electron initially

launched along a Kepler orbit turns chaotic, leading to an efficient energy absorption also on the quantum level, which finally leads to the ionization of the atom. Hence, we define the electronic survival probability as the remaining bound state population after an interaction time t , with \mathcal{P}_Ω the projector on the bound state component of Hilbert space. The Γ_j in Eq. (1) then become the ionization rates of the Floquet eigenstates $|\epsilon_j\rangle$ of the atom in the field, and the ω_j the associated overlaps (averaged over one field cycle [6]) of $|\phi_0\rangle$ with $|\epsilon_j\rangle$. With some theoretical and numerical effort, all these quantities can be extracted from the fundamental Floquet eigenvalue problem, for typical parameter values of state of the art laboratory experiments [13].

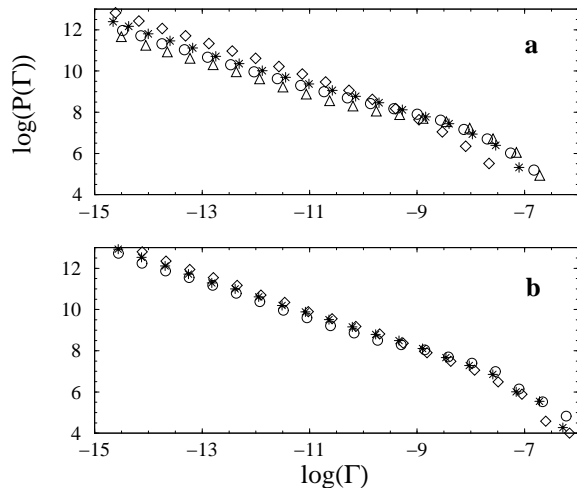


FIG. 1. Distribution of the ionization rates Γ of microwave-driven (a) 1D and (b) 3D $m_0 = 0$ Rydberg states of atomic hydrogen, for three different values of the localization parameter $\mathcal{L} = 0.25$ (diamonds), 0.5 (stars), 1.0 (circles), and 2.0 (pyramids; only in (a), because of the high cost of 3D calculations at the corresponding high field amplitudes). The distributions were generated, at fixed \mathcal{L} , by sampling the Floquet spectra over the frequency (and corresponding amplitude, F) ranges $\omega/2\pi = 13.16 \dots 16.45$ GHz (1D) and $35.5 \dots 36.1$ GHz (3D), within a Floquet zone of width ω centered around $n_0 = 70$ (3D) and 100 (1D), respectively.

The atomic ionization process is mapped on the Anderson model through the atomic localization parameter $\mathcal{L} = \xi/\eta$ [2], with ξ the localization length in units of the photon energy. η is the ionization potential of $|\phi_0\rangle$, measured in units of ω , and is completely determined by n_0 , due to the angular momentum degeneracy of the hydrogen spectrum. Provided that n_0 – through its correspondence with the principal action of the classical dynamics – is chosen within the chaotic component of phase space (possibly garnished by nonlinear resonance islands and remnants of classically regular motion immersed in the “chaotic sea”), η can be conceived as a measure of the extension of the domain of complex transport along the energy axis. If we identify η with the sample length in the original Anderson problem and average over different

realizations of a fixed value of $\mathcal{L} \ll 1$, quantum suppression of transport through exponentially localized eigenfunctions over the quasi-resonantly coupled states on the energy axis [2,7,14] implies a distribution $P(\Gamma) \sim 1/\Gamma$ of the ionization rates entering Eq. (1), in accord with the current theory [11] on open Anderson insulators.

Statistically independent realizations of a fixed localization parameter can be generated by simultaneous variation of F and ω , due to the relation $\mathcal{L} \simeq 6.66F^2n_0^2/\omega^{7/3}$ from the original theory on dynamical localization [2] in periodically driven, one dimensional hydrogen atoms. Whilst this theory has no quantitative predictive power [6,12], it is nonetheless known to give qualitatively correct predictions, even for 3D Rydberg states with not too large values of the angular momentum quantum number ℓ . In the sequel we therefore use this quantity such as to guide our choice of F and ω values.

Fig. 1 shows the distribution of ionization rates Γ of real 3D hydrogen Rydberg states and of a one dimensional model atom (where the Rydberg electron is confined to 1D configuration space $z > 0$ defined by the polarization axis, with the Coulomb singularity at the origin [6,9]) exposed to a microwave field, within a Floquet zone (of width ω on the energy axis [6,13]) centered around the $n_0 = 70$ (3D) and $n_0 = 100$ (1D) Rydberg manifold. The different values of $\mathcal{L} = 0.25 \dots 2.0$ are realized by sampling the spectra over frequency ranges $\omega/2\pi = 35.5 \dots 36.1$ GHz (3D), and $13.16 \dots 16.45$ GHz (1D), respectively, and adjusting F correspondingly. Due to the dramatically enhanced spectral density of the 3D as compared to the 1D problem (a consequence of the additional degree of freedom labeled by ℓ) only ten equidistant ω -values are needed to generate the 3D data (with a total sample size of approx. 25000 eigenstates), in contrast to 500 in the 1D case (up to 100000 eigenvalues).

For small localization parameter $\mathcal{L} = 0.25$, both, the 1D model atom as well as the real object do exhibit ionization rates distributed according to the Γ^{-1} law, over approx. seven orders of magnitude from $\Gamma \simeq 10^{-15}$ to $\Gamma \simeq 10^{-9}$ a.u., in nice agreement with the prediction for decay from a disordered solid [11]. However, as the localization parameter is increased (by systematically increasing F over the entire frequency range indicated above) to $\mathcal{L} = 1.0$, we observe a depletion of the distribution at small rates, balanced by a decrease of the slope of $P(\Gamma)$ in an intermediate range $\Gamma \simeq 10^{-10} \dots 10^{-8}$ a.u. Such behavior is clearly incompatible with the simple picture of exponentially localized probability densities along the energy axis (due to dynamical localization of the eigenstates over the chaotic phase space component) [2,7,14], and suggests the presence of alternative transport mechanisms which compete with dynamically localized diffusion [9,10]. As already anticipated in the introduction, such observation does not come as a surprise, since periodically driven Rydberg states exhibit a mixed regular chaotic phase space. Indeed, it is known from experimental as well as exact theoretical/numerical studies [9,12,15] of strongly perturbed atomic Rydberg systems,

and, more recently, from mesoscopic systems with decay [10], that the eigenstates of such quantum systems can be classified according to their localization [9,10,16] (i) on regular and/or elliptic regions, (ii) along remnants of regular motion immersed in the chaotic sea (“separatrix/hierarchical states” living on “can-tori”), and (iii) in the chaotic domain of phase space. Furthermore, elliptic regions as well as remnants of invariant tori are rather robust under changes of some control parameter such as F in our present case [9].

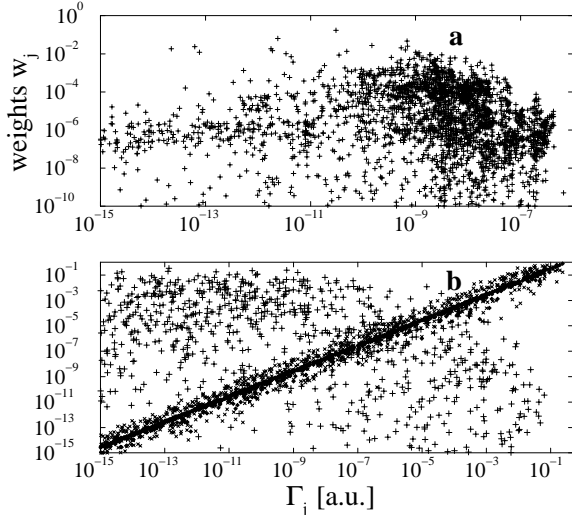


FIG. 2. (a) Expansion coefficients w_j of the 3D atomic initial state $|n_0 = 70, \ell_0 = 0, m_0 = 0\rangle$ in the Floquet eigenstates $|\epsilon_j\rangle$, for $\mathcal{L} = 1.0$ and $\omega/2\pi = 35.6$ GHz, vs. the associated decay rates Γ_j . (Qualitatively similar results are obtained for the one dimensional model atom, as well as for microwave driven alkali Rydberg states [17].) (b) Same as (a), but for initial states prepared at the sites 900 (plusses), 999 (crosses), 1000 (diamonds clustered along the diagonal) of a 1D Anderson model of sample length $N = 1000$ (uniformly distributed on-site potentials V_{n_i} with $|V_{n_i}| \leq 1.5$, constant coupling $V_{n_i, n_i \pm 1} = 1$, and an absorbing boundary at one end, introduced by adding an imaginary part $-i\gamma = -i \times 0.31$ to the on-site potential at $n_i = 1000$; results for 10 realizations of the potential are gathered together). Only in the special case of the initial state placed right at the edge $n_i = 1000$ of the sample is there a one-to-one relation between decay rates and expansion coefficients!

Accordingly, the localization properties as well as the decay rates of the associated eigenstates tend to be less sensitive when changing F , whereas those states localized in the chaotic domain, with their decay rates essentially determined by \mathcal{L} , exhibit rapidly increasing rates as F is increased. Hence, we attribute the deviation from the Γ^{-1} law at large values of F in Fig. 1 to the rapid increase of the decay rates of class (iii) states with \mathcal{L} (corresponding to the effective destruction of dynamical localization), whereas class (i) and (ii) states accumulate at intermediate Γ -values at the largest \mathcal{L} -values considered here (we verified this assertion by inspection of the Husimi phase

space representations of the Floquet eigenstates of the 1D problem [9]). At small values of \mathcal{L} , the latter exhibit extremely small ionization rates below $\Gamma \simeq 10^{-13}$ a.u. (or even below $\Gamma \simeq 10^{-15}$ a.u., this is below our numerical precision, hence the plot does not extend into that domain), what leads to isolated, extremely narrow resonances in experimental or numerical photoionization cross sections [9,15]. Therefore, in this parameter regime, $P(\Gamma)$ is dominated by the decay rates of the dynamically localized class (iii) states, in agreement with the Anderson scenario. Let us also comment on the apparently distinct weight of class (i) and (ii) states in the 1D and the 3D situation, which is born out in Fig. 1: the depletion of the low- Γ part is less pronounced for the real atom, and equally so the region of decreased slope at intermediate Γ -values. This is due to the contribution of high ℓ states (at fixed m_0) to the rate distribution – unavailable in 1D – which exhibit vanishing decay rates and do not contribute to the plotted distribution at small \mathcal{L} . As \mathcal{L} is increased, these states contribute to $P(\Gamma)$ in the range $\Gamma < 10^{-11}$ a.u., such as to compensate for the reshuffling of low- ℓ states from small to intermediate Γ 's. This smooths the 3D distribution as compared to the 1D result.

Hence, we have seen how chaotic transport can mimic signatures of disorder in the quantum decay rate distribution, and induce amendments thereof due to peculiar structures of mixed regular chaotic dynamics. As obvious from Eq. (1), $P(\Gamma)$ does not determine the (experimentally often very easily accessible [6,9,13]) survival probability alone, but only in conjunction with the expansion coefficients w_j . Starting from a general form $P(\Gamma) \sim \Gamma^{-\alpha}$, many authors infer a “universal” time dependence $P_{\text{surv}} \sim 1/t^{2-\alpha}$, leaning on the additional assumption $w_j \sim \Gamma_j$ [7,8]. The latter is nonetheless *only* justified if the initial state $|\phi_0\rangle$, which represents a *local* probe of the spectrum, is localized close to the boundary of Ω – which is the “edge of the sample” in a language adapted to the Anderson scenario, and the ionization threshold $n \rightarrow \infty$ in the atomic problem. For a generic choice of $|\phi_0\rangle$ “within the sample”, i.e. somewhere within Ω , this basic assumption is utterly misleading, as illustrated in Fig. 2. In Fig. 2 a), we show the distribution of the w_j and of the corresponding Γ_j , on a *double logarithmic* plot, for $|\phi_0\rangle = |n_0 = 70, \ell_0 = 0\rangle$ in driven 3D hydrogen. The essentially uncorrelated w_j and Γ_j nicely correlate with the earlier finding that phase space localization properties and decay rates of strongly driven Rydberg atoms are *not* unambiguously related [9], and clearly devalidate the above proportionality assumption. On the other hand, it can easily be shown within a simple, one dimensional Anderson model how the generic situation of Fig. 2 a) continuously evolves into the situation of strongly correlated w_j and Γ_j , as illustrated in Fig. 2 b): There, we calculated the decay rates of the eigenstates of a 1D tight binding Hamiltonian of length $N = 1000$, with diagonal disorder and constant off-diagonal terms. Decay is introduced in this model by absorbing bound-

ary conditions at one end, whereas a reflecting wall is imposed at the other. If $|\phi_0\rangle$ is placed well inside the sample, expansion coefficients and decay rates are uncorrelated, though the distribution collapses onto a straight line $w_j \sim \Gamma_j$ as $|\phi_0\rangle$ is shifted towards the open end (site $n_i = 1000$) of the sample. It is this latter situation which was realized in recent numerical calculations on periodically driven hydrogen atoms additionally subjected to an intense static electric field [7].

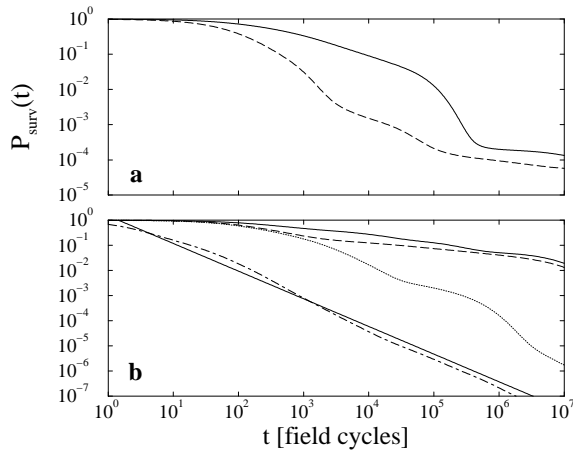


FIG. 3. Survival probability $P_{\text{surv}}(t)$ obtained from distributions as in Figs. 1 and 2 via Eq. (1). (a) 1D hydrogen, initial state $|n_0 = 100\rangle$, driving frequencies and localization parameters $\omega/2\pi = 16.45$ GHz, $\mathcal{L} = 1.0$ (full line), 13.16 GHz and 2.0 (dashed); (b) 3D hydrogen, $n_0 = 70$, $m_0 = 0$, $\ell_0 = 0$ (solid line), 15 (dashed), 45 (dotted), $\omega/2\pi = 35.6$ GHz, $\mathcal{L} = 1.0$. In this latter case, different w_j -distributions are realized by changing the angular momentum ℓ_0 of the initial atomic state, always leading to near-algebraic decay (like in 1D), though with distinct (and *non-universal*) decay exponents. Only fictitious expansion coefficients $w_j \equiv \Gamma_j / \langle \Gamma \rangle$ induce asymptotically “universal” decay $P_{\text{surv}}(t) \sim t^{-\gamma}$ (dash-dotted line), $\gamma \approx 2 - \alpha \approx 1.1$ (indicated by the full line), with $\Gamma_j, \langle \Gamma \rangle$, and $\alpha \approx 0.9$ extracted from the $\Gamma < 10^{-10}$ a.u. part of the $\mathcal{L} = 1.0$ data in Fig. 1(b).

Given the results illustrated in Fig. 2, we can no more hope for a universal decay law for the survival probability $P_{\text{surv}}(t)$ – despite the rather universal features of $P(\Gamma)$. This is finally illustrated in Fig. 3, where we show $P_{\text{surv}}(t)$ for 1D and 3D hydrogen in the case of large \mathcal{L} : Whilst algebraic decay of $P_{\text{surv}}(t) \sim t^{-\gamma}$ is generic (even if modulated by local fluctuations [18]), simply due to the broad distribution of the w_j and Γ_j as illustrated in Figs. 1 and 2, the “universal” decay exponent $\gamma = 2 - \alpha$ is only observed in accidental cases – or if we reshuffle the expansion coefficients of Fig. 2 a) according to $w_j \rightarrow \Gamma_j / \langle \Gamma \rangle$, with $\langle \Gamma \rangle$ the average rate over the entire spectrum, as illustrated in Fig. 3 b). In this, however, unrealistic case, $P_{\text{surv}}(t)$ asymptotically decays with $\gamma \approx 1.1$, which perfectly matches the prediction $\gamma = 2 - \alpha$, with $\alpha = 0.9$ extracted from the small Γ ($< 10^{-10}$ a.u.) part of the corresponding data set in Fig. 1 b). Therefore, universal

features of the statistics of the decay rates of classically chaotic quantum systems do generically *not* carry over to the time dependent decay of the survival probability of some initial state prepared at an arbitrary location in phase space. This simply expresses the essential decorrelation of the phase space localization properties of the eigenstates of chaotic quantum systems and of their asymptotics – which *alone* determine their decay.

Support from EU Program QTRANS RTN1-1999-08400, is gratefully acknowledged (S.W.).

-
- [1] S. Fishman, D. R. Grempel, and R. E. Prange, Phys. Rev. Lett. **49**, 509 (1982).
 - [2] G. Casati, I. Guarneri, and D. L. Shepelyansky, IEEE J. Quant. Electron. **24**, 1420 (1988).
 - [3] R.S. MacKay, J.D. Meiss, and I.C. Percival, Phys. Rev. Lett. **52**, 697 (1984).
 - [4] T. Geisel, G. Radons, and J. Rubner, Phys. Rev. Lett. **57**, 2883 (1986).
 - [5] M. Reed and B. Simon, *Methods of Modern Mathematical Physics IV: Analysis of Operators*, Academic Press, San Diego (1980).
 - [6] A. Buchleitner, D. Delande, and J.-C. Gay, J. Opt. Soc. Am. B **12**, 505 (1995).
 - [7] G. Benenti *et al.*, Phys. Rev. Lett. **84**, 4088 (2000).
 - [8] A. Ossipov *et al.*, Phys. Rev. B **64**, 224210 (2001).
 - [9] A. Buchleitner, Ph.D. thesis, Université Pierre et Marie Curie, Paris, 1993; A. Buchleitner and D. Delande, Chaos, Solitons & Fractals **5**, 1125 (1995); Phys. Rev. Lett. **75**, 1487 (1995); A. Buchleitner *et al.*, Phys. Rev. Lett. **75**, 3818 (1995).
 - [10] R. Ketzmerick *et al.*, Phys. Rev. Lett. **85**, 1214 (2000).
 - [11] M. Terraneo and I. Guarneri, Eur. Phys. J. B **18**, 303 (2000).
 - [12] P.M. Koch and K.A.H. Leeuwen, Phys. Rep. **255**, 289 (1995).
 - [13] A. Krug and A. Buchleitner, Phys. Rev. Lett. **86**, 3538 (2001).
 - [14] G. Casati, G. Maspero, and D. L. Shepelyansky, Phys. Rev. Lett. **82**, 524 (1999).
 - [15] B. Grémaud, D. Delande, and J.-C. Gay, Phys. Rev. Lett. **70**, 1615 (1993).
 - [16] G.P. Berman and G.M. Zaslavsky, Phys. Lett. **61A**, 295 (1977); S.W. MacDonald and A.N. Kaufman, Phys. Rev. Lett. **42**, 1189 (1979); J.G. Leopold and D. Richards, J. Phys. B **27**, 2169 (1994).
 - [17] A. Krug, PhD thesis, Ludwig-Maximilians-Universität München, 2001, available at www.ub.uni-muenchen.de/elektronische_dissertationen/physik/Krug-Andreas.pdf.
 - [18] S. Wimberger and A. Buchleitner, J. Phys. A **34**, 7181 (2001).